A&A 402, L9–L12 (2003)
DOI: 10.1051/0004-6361:20030371

Astronomy & Astrophysics

The afterglow of GRB 021211: Another case of reverse shock emission

D. M. Wei⋆

Purple Mountain Observatory, Chinese Academy of Sciences, Nanjing, PR China
National Astronomical Observatories, Chinese Academy of Sciences, PR China

Received 17 January 2003 / Accepted 12 March 2003

Abstract. GRB 021211 was first detected by HETE II and its early afterglow has been observed. There is a break in its afterglow light curve at about 12 min after the bursts, before the break the optical flux decays with a power-law index of about −1.6, while at late time the power-law slope is about −1 (Chornock et al. 2002). Here we will show that the afterglow light curve of GRB 021211 can be explained within the framework of the standard fireball model. We show that the afterglow emission before the break time is the contribution of the emission from both the reverse shock and the forward shock, while the afterglow emission after the break time is mainly due to the forward shock emission. From the fitting we can give constraints on the parameters: the initial Lorentz factor $250 \leq \gamma_0 \leq 900$, and the surrounding medium density $n \geq 1.6 \times 10^{-3}$ atoms cm^{-3}. We propose that since the values of ϵ_B and ϵ_e are somewhat smaller for GRB 021211, so the peak energy of the reverse shock emission is well below the optical band, and thus it is substantially fainter than 990123 at similar epochs. Also we suggest that such a break might be a common feature in early optical afterglows.

Key words. gamma rays: bursts

1. Introduction

GRB 021211 is a bright, long gamma-ray burst detected by HETE II on 2002 December 11 at 11:18:34 UT. The burst duration in the 8–40 keV band was >5.7 s, the fluence was about 1×10^{-6} ergs cm^{-2} and the peak flux was $>8 \times 10^{-7}$ ergs cm^{-2} s^{-1} (Crew et al. 2002). This burst was also observed by Ulysses and Konus-Wind. As observed by Ulysses, it had a duration of about 15 s, a 25–100 keV fluence was approximately 1.8×10^{-6} erg cm^{-2}, and a peak flux was about 4.5×10^{-7} erg cm^{-2} s^{-1} (Hurley et al. 2002). The spectroscopic observations of the optical afterglow identified three emission lines as [OII] 3727, and [OIII] 4959, 5007 at a redshift of $z = 0.800 \pm 0.001$ (Vreeswijk et al. 2002). Assuming $\Omega_m = 0.3$, $\Omega_\Lambda = 0.7$, and $h = 0.65$, the isotropic gamma-ray energy is $\sim 3.2 \times 10^{51}$ ergs.

The prompt localization of GRB 021211 by HETE II allowed the rapid follow-up observation of the afterglow at very early time. Several groups had detected the optical emission shortly after the gamma-ray burst (Park et al. 2002; Li et al. 2002; Wozniak et al. 2002). The observations show that the optical flux declined steeply at early time, with a power-law index of about −1.6, while at later time the flux decayed with a slope of about −1, the break time is about 12 min after the burst (Chornock et al. 2002).

This break from a steep initial decline to a shallow later decline is similar to the early behavior of GRB 990123 (Akerlof et al. 1999). The early emission of GRB 990123 is believed to be due to the reverse shock, while the later emission is ascribed to the normal forward shock (Sari & Piran 1999a). Recently Kobayashi & Zhang (2003) have shown that the rebrightening in the GRB 021004 optical afterglow light curve can be explained by the reverse shock and forward shock. Here we will show that this early break around 12 min after the burst can be interpreted as the superposition of the reverse shock and forward shock emission.

2. The emission from forward shock and reverse shock

2.1. Forward shock

Multiwavelength follow-up of gamma-ray burst afterglows has revolutionized GRB astronomy in recent years, yielding a wealth of information about the nature of GRBs. The observed properties of GRB afterglows are broadly consistent with models based on relativistic blast waves at cosmological distances (Meszaros & Rees 1997; Wijers et al. 1997). In the standard fireball models, the huge energy released by an explosion ($\sim 10^{52}$ ergs) is converted into kinetic energy of a shell expanding at ultra-relativistic speed. After the main GRB event occurred, the fireball continues to propagate into the surrounding gas, driving an ultra-relativistic blast wave (forward shock) into the ambient medium. The forward shock continuously heats fresh gas and accelerates relativistic electrons to very high

⋆ e-mail: dmwei@pmo.ac.cn

energy, which produce the afterglow emission through synchrotron radiation.

Sari et al. (1998) have discussed the emission features of forward shock in great details. Using their results, we have

$$\nu_{\rm m,f} = 5.1\times10^{15}\,(1+z)^{1/2}\,\epsilon_{\rm B}^{1/2}\epsilon_{\rm e}^{2}g^{2}E_{52}^{1/2}t_{\rm d}^{-3/2}\quad {\rm Hz} \tag{1}$$

$$\nu_{\rm c,f} = 2.7\times10^{12}\,(1+z)^{-1/2}\,\epsilon_{\rm B}^{-3/2}E_{52}^{-1/2}n^{-1}t_{\rm d}^{-1/2}\quad {\rm Hz} \tag{2}$$

$$t_{\rm m,f} = 2.9\,(1+z)^{1/3}\,\epsilon_{\rm B}^{1/3}\epsilon_{\rm e}^{4/3}g^{4/3}E_{52}^{1/3}\nu_{\rm R,15}^{-2/3}\quad {\rm days} \tag{3}$$

$$t_{\rm c,f} = 7.3\times10^{-6}\,(1+z)^{-1}\,\epsilon_{\rm B}^{-3}E_{52}^{-1}n^{-2}\nu_{\rm R,15}^{-2}\quad {\rm days} \tag{4}$$

$$F_{\nu,\rm max,f} = 110\,(1+z)\,\epsilon_{\rm B}^{1/2}E_{52}n^{1/2}D_{28}^{-2}\quad {\rm mJy} \tag{5}$$

where $\nu_{\rm m,f}$ is the typical synchrotron frequency of forward shock emission, $\nu_{\rm c,f}$ is the cooling frequency, $\epsilon_{\rm B}$ and $\epsilon_{\rm e}$ are the fractions of the shock energy transferred to the magnetic field and electrons, $g = (p-2)/(p-1)$, p is the index of electron energy distribution, E_{52} is the burst energy in units of 10^{52} ergs, $t_{\rm d}$ is the observer's time in units of 1 day, n is the surrounding medium density in units of 1 atom cm^{-3}, $\nu_{\rm R,15} = \nu_{\rm R}/10^{15}$ Hz, D_{28} is the luminosity distance in units of 10^{28} cm, $t_{\rm m,f}$ ($t_{\rm c,f}$) is the time when the frequency $\nu_{\rm m,f}$ ($\nu_{\rm c,f}$) crosses the observed optical frequency, and $F_{\nu,\rm max,f}$ is the peak flux.

According to the fireball model, before the peak time $t_{\rm m,f}$, the observed optical flux is expected to increase as $F_\nu \propto t^{1/2}$, when the typical synchrotron frequency crosses the observed optical band, the flux reaches the maximum flux $F_{\nu,\rm max,f}$, and then when $t > t_{\rm m,f}$, the flux decays as $F_\nu \propto t^{-3(p-1)/4}$.

2.2. Reverse shock

The emission of reverse shock have been discussed by Meszaros & Rees (1997) and Sari & Piran (1999b). This shock heats up the shell's matter and accelerates its electrons, then these electrons loss energy through synchrotron radiation. The reverse shock and the forward shock are separated by a contact discontinuity, across which the pressure is equal, so the energy density in both shocked regions is the same, therefore the total energy in both shocks is comparable.

The typical synchrotron frequency $\nu_{\rm m,r}$ and cooling frequency $\nu_{\rm c,r}$ of the reverse shock at the time when it crosses the shell can be easily calculated by comparing them to those of the forward shock. Since at the shock crossing time ($t_{\rm A}$), the reverse shock and the forward shock have the same Lorentz factor and energy density (which suggests the magnetic fields in both shocked regions are the same, if we assume that the magnetic equipartition factor is same in both regions), so the cooling frequency of the reverse shock $\nu_{\rm c,r}$ is the same as that of the forward shock,

$$\nu_{\rm c,r}(t_{\rm A}) \simeq \nu_{\rm c,f}(t_{\rm A}). \tag{6}$$

The typical synchrotron frequency is proportional to the electrons random Lorentz factor squared and to the magnetic field and to the Lorentz boost. The Lorentz boost and the magnetic field are the same for both the reverse shock and forward shock, while the random Lorentz factor of reverse shock is $\gamma_0/\gamma_{\rm A}$ compared to $\gamma_{\rm A}$ of the forward shock, i.e. the effective temperature of reverse shock is much lower than that of the forward shock (by a factor $\gamma_{\rm A}^2/\gamma_0$, where γ_0 is the initial Lorentz factor and $\gamma_{\rm A}$ is the Lorentz factor at the crossing time), then the typical synchrotron frequency of reverse shock at the crossing time is

$$\nu_{\rm m,r}(t_{\rm A}) \simeq \frac{\gamma_0^2}{\gamma_{\rm A}^4}\nu_{\rm m,f}(t_{\rm A}) \tag{7}$$

$$\simeq 3.5\times10^{15}\epsilon_{\rm B}^{1/2}\left(\frac{\epsilon_{\rm e}}{0.1}\right)^2 g^2\left(\frac{\gamma_0}{300}\right)^2 n^{1/2}\,{\rm Hz}. \tag{8}$$

The peak flux at the typical frequency is proportional to the number of electrons, the magnetic field and the Lorentz boost. The magnetic fields and the Lorentz boost are the same for both reverse and forward shock, while at the crossing time the mass of the shell is larger by a factor of $\gamma_{\rm A}^2/\gamma_0$ than that of the ambient medium swept by the forward shock (Kobayashi & Zhang 2003), so we have

$$F_{\nu,\rm max,r}(t_{\rm A}) \approx \frac{\gamma_{\rm A}^2}{\gamma_0}F_{\nu,\rm max,f} \tag{9}$$

$$\approx 110\,(1+z)\,\frac{\gamma_{\rm A}^2}{\gamma_0}\epsilon_{\rm B}^{1/2}E_{52}n^{1/2}D_{28}^{-2}\ {\rm mJy}. \tag{10}$$

After the reverse shock has passed through the ejecta, the ejecta cools adiabatically. Sari & Piran (1999a) have shown that, for $t > t_{\rm A}$, the particle Lorentz factor evolves as $\gamma_{\rm e} \propto t^{-13/48}$, the emission frequency drops quickly with time according to $\nu_{\rm e} \propto t^{-73/48}$, and the peak flux falls like $F_{\nu_{\rm e}} \propto t^{-47/48}$. So if the optical band $\nu_{\rm R}$ is below the typical synchrotron frequency $\nu_{\rm m,r}$, then the flux decays as $F_\nu \propto t^{-17/36}$, while when $\nu_{\rm R} > \nu_{\rm m,r}$, the flux decreases as $F_\nu \propto t^{-(21+73p)/96}$.

3. Fitting the afterglow of GRB 021211

Using the emission features of reverse shock and forward shock described above, we can fit the optical light curve of GRB 021211. Here we take the values $z = 0.8$, $E = 3.2\times10^{51}$ ergs, and $p = 2.3$.

For the forward shock emission, the observed optical flux is

$$\frac{F_{\nu,\rm f}(t)}{F_{\nu,\rm max,f}} = \begin{cases} \left(\frac{t}{t_{\rm m,f}}\right)^{1/2} & \text{for}\quad t < t_{\rm m,f} \\ \left(\frac{t}{t_{\rm m,f}}\right)^{-3(p-1)/4} & \text{for}\quad t_{\rm m,f} < t < t_{\rm c,f}. \end{cases} \tag{11}$$

Using Eqs. (3), (5) and (11) we can give the afterglow light curve from the forward shock, as shown in Fig. 1 by the dashed line. From fitting the observed data we can obtain the relation

$$\epsilon_{\rm B}\left(\frac{\epsilon_{\rm e}}{0.1}\right)^{8/5} n^{3/5} \sim 9.1\times10^{-4}. \tag{12}$$

In addition, the observation implies that $t_{\rm m,f}$ should be less than 100 s (if $t_{\rm m,f} > 100$ s, there will be a bump in the afterglow light curve), and $t_{\rm c,f}$ should be larger than 1 day (otherwise there will be a steepening of the light curve), so from Eqs. (3), (4) we have

$$\epsilon_{\rm B}^{1/4}\left(\frac{\epsilon_{\rm e}}{0.1}\right) \le 0.14 \tag{13}$$

$$\epsilon_{\rm B}n^{2/3} \le 0.04. \tag{14}$$

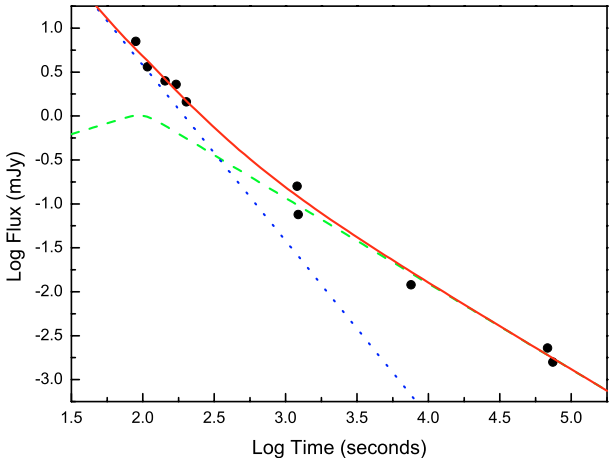

Fig. 1. The optical light curve of GRB 021211. The dashed line is the emission of the forward shock, the dotted line represents the emission from reverse shock, and the solid line is the total flux. Data from: Price & Fox (2002a, 2002b), Park et al. (2002), Li et al. (2002), Kinugasa et al. (2002), McLeod et al. (2002), Wozniak et al. (2002), Levan et al. (2002).

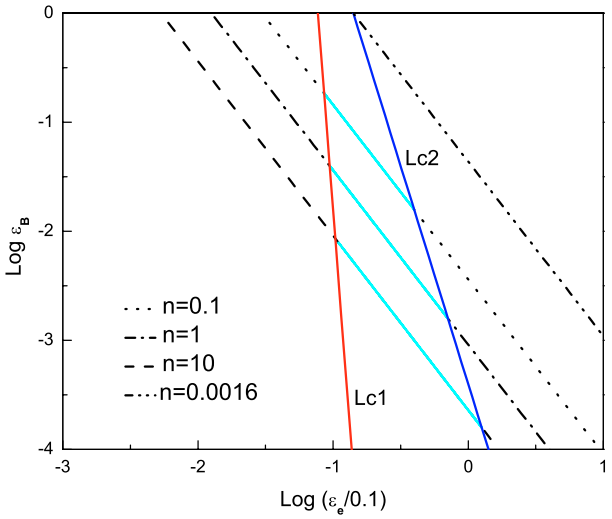

Fig. 2. The relation between ϵ_B, ϵ_e and n given by Eqs. (12), (13) and (19). The dotted, dash-dotted, dashed and dot-dot-dashed lines represent n = 0.1, 1, 10 and 0.0016 respectively. The allowed values of ϵ_B and ϵ_e lie in the region confined by two lines Lc1 (Eq. (19)) and Lc2 (Eq. (13)).

For the reverse shock emission, for $t > t_A$, we have the relations $\nu_{m,r}(t) = \nu_{m,r}(t_A)\left(\frac{t}{t_A}\right)^{-73/48}$, $F_{\nu,max,r}(t) = F_{\nu,max,r}(t_A)\left(\frac{t}{t_A}\right)^{-47/48}$, then the observed flux can be written as

$$F_{\nu,r}(t) = F_{\nu,max,r}(t)\left[\frac{\nu}{\nu_{m,r}(t)}\right]^{-(p-1)/2} \quad (15)$$

$$= F_{\nu,max,r}(t_A)\left[\frac{\nu}{\nu_{m,r}(t_A)}\right]^{-\frac{(p-1)}{2}}\left(\frac{t}{t_A}\right)^{-\frac{73p+21}{96}}. \quad (16)$$

Using Eqs. (8), (10) and (16) we can give the afterglow light curve from the reverse shock, as shown in Fig. 1 by the dotted line. From fitting we can obtain the relation

$$\left(\frac{\gamma_0}{300}\right)^{23/10}\left(\frac{\gamma_A}{\gamma_0}\right)^2 \epsilon_B^{33/40}\left(\frac{\epsilon_e}{0.1}\right)^{13/10} n^{33/40} t_A^2 \sim 9.8. \quad (17)$$

Combining Eqs. (12), (14) and (17), we get

$$\left(\frac{\gamma_0}{300}\right)\left(\frac{\gamma_A}{\gamma_0}\right)^{20/23} \sim 31\epsilon_B^{-1/184} n^{-27/184} t_A^{-20/23} \quad (18)$$

$$\epsilon_B^{1/16}\left(\frac{\epsilon_e}{0.1}\right) \geq 0.077. \quad (19)$$

Therefore Eqs. (12), (13) and (19) give the constraint on the parameters ϵ_B, ϵ_e and n. Figure 2 shows the relation between ϵ_B, ϵ_e and n. The dotted, dash-dotted, dashed and dot-dot-dashed lines represent n = 0.1, 1, 10 and 0.0016 respectively. We find that the allowed values of ϵ_B and ϵ_e lie in the region confined by two lines Lc1 (Eq. (19)) and Lc2 (Eq. (13)). It is obvious that n must be larger than 0.0016, and ϵ_e must be larger than 0.0077. If we take $n = 1$, $\epsilon_e = 0.07$, then $\epsilon_B = 1.6 \times 10^{-3}$. We propose that more observations are needed in order to further estimate the values of ϵ_B, ϵ_e and n.

From Eq. (18) we see that the initial Lorentz factor γ_0 depends on ϵ_B and n very weakly, so as an approximation, and taking $\gamma_A \sim \gamma_0$, then we have $\gamma_0 \sim 9300 t_A^{-20/23}$. Since the duration is about 15 s and the first observation time is 65 s after the burst, so the value of t_A should lie between 15 s and 65 s, and therefore we can get the initial Lorentz factor $250 < \gamma_0 < 900$, which is consistent with the lower limit estimates base on the γ–γ attenuation calculation (Fenimore et al. 1993).

4. Discussion and conclusion

The current afterglow observations usually detect radiation several hours after the burst, at this stage the Lorentz factor is independent of the initial Lorentz factor, thus these observations do not provide useful information on the initial extreme relativistic motion. The initial Lorentz factor is a very important quantity for constraining the GRB models since it specifies how "clean" the fireball is. Therefore to detect the early afterglow of GRBs is very important, since it can provide the information on the initial Lorentz factor. It is fortunately that the early afterglow of GRB 021211 have been observed, by fitting its optical light curve we obtain its initial Lorentz factor $250 < \gamma_0 < 900$, this value seems reasonable since it is widely believed that the initial fireball Lorentz factor should be larger than 100 in order to avoid photon-photon attenuation. Of course, further constraint on the value of γ_0 needs more early afterglow observations.

GRB 990123 is the first burst for which its optical flash was observed, the peak flux was about 1 Jy in R-band. After that many efforts have been made to try to find the optical flash from other GRBs, but only upper limits are given (Akerlof et al. 2000). Here we also note that the optical flux of GRB 021211 is substantially fainter than 990123 at similar epochs. Why GRB 990123 is so bright? One reason may be that GRB 990123 is a very bright burst, so its reverse shock emission is also very strong. On the other hand, from fitting we note that the values of ϵ_B and ϵ_e of GRB 021211 are somewhat smaller, which leads to the fact that the typical synchrotron frequency of reverse shock is well below the optical band, so the early afterglow (or optical flash) is weak. While for GRB 990123 the typical

synchrotron frequency of reverse shock is close to the optical band (Sari & Piran 1999a; Kobayashi & Zhang 2003).

For smaller values of ϵ_B and ϵ_e, not only the typical synchrotron frequency of reverse shock is small, but also the typical synchrotron frequency of forward shock is small, so the time $t_{m,f}$ when the typical frequency of forward shock crosses the optical band is also small, for GRB 021211, the observations required $t_{m,f} \leq 100$ s. The late time afterglow for $t > t_{m,f}$ is $F_\nu = F_{\nu,max,f}\,(t/t_{m,f})^{-3(p-1)/4}$, so for smaller value of $t_{m,f}$, the observed optical flux should be much fainter than those with larger values of $t_{m,f}$, so we suggest that the so-called dark bursts whose afterglow have not been observed might be due to their very small values of $t_{m,f}$.

The early afterglow of GRB 021211 shows that there is a early break in its optical light curve, before the break time the flux declined with a power-law index of about -1.6, while at later time the flux decayed with a slope of about -1. Although the reverse shock model predicts that the optical flux should decay with a power-law index of about -2, here we show that the superposition of both the forward shock and the reverse shock emission can well account for the observed light curve. Therefore we suggest that this early break might be a common feature in early optical afterglow, and before the break time the slope of flux decline may be flatter than -2 since it contains the contribution from both the reverse shock and the forward shock emission.

Acknowledgements. This work is supported by the National Natural Science Foundation (grants 10073022 and 10225314) and the National 973 Project on Fundamental Researches of China (NKBRSF G19990754).

References

Akerlof, C., Balsano, R., Barthelemy, S., et al. 1999, Nature, 398, 400
Akerlof, C., Balsano, R., Barthelemy, S., et al. 2000, ApJ, 532, L25
Chornock, R., Li, W., Filippenko, A. V., & Jha, S. 2002, GCN, 1754
Crew, G., Villasenor, J., Vanderspek, R., et al. 2002, GCN, 1734
Fenimore, E. E., Epstein, R. I., & Ho, C. 1993, A&AS, 97, 59
Hurley, K., Mazets, E., Golenetskii, S., & Cline, T. 2002, GCN, 1755
Kinugasa, K., Kato, T., Yamaoka, H., & Torii, K. 2002, GCN, 1749
Kobayashi, S., & Zhang, B. 2003, ApJ, 582, L75
Levan, A., Fruchter, A., Welch, D., et al. 2002, GCN, 1758
Li, W., Filippenko, A. V., Chornock, R., & Jha, S. 2002, GCN, 1737
McLeod, B., Caldwell, N., Grav, T., et al. 2002, GCN, 1750
Meszaros, P., & Rees, M. J. 1997, ApJ, 476, 231
Park, H. S., Williams, G., & Barthelmy, S. 2002, GCN, 1736
Price, P. A., & Fox, D. W. 2002a, GCN, 1732
Price, P. A., & Fox, D. W. 2002b, GCN, 1733
Sari, R., Piran, T., & Narayan, R. 1998, ApJ, 497, L17
Sari, R., & Piran, T. 1999a, ApJ, 517, L109
Sari, R., & Piran, T. 1999b, ApJ, 520, 641
Vreeswijk, P., Burud, I., Fruchter, A., & Levan, A. 2002, GCN, 1756
Wijers, A. M. J., Rees, M. J., & Meszaros, P. 1997, MNRAS, 288, L51
Wozniak, P., Vestrand, W. T., Starr D., et al. 2002, GCN, 1757